

Contrasting Nanoscale Surface Morphologies of Polyurethanes Containing Polyoxetane Soft Blocks with Random and Block Segmer Sequences

Tomoko Fujiwara and Kenneth J. Wynne*

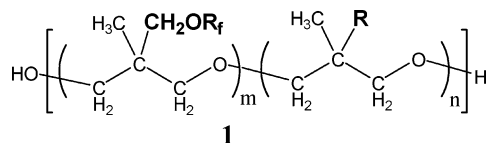
Department of Chemical Engineering, Virginia Commonwealth University, Richmond, Virginia 23284-3028

Received June 23, 2004

Revised Manuscript Received September 20, 2004

Control of polymer surface chemistry and morphology is the subject of continuing fundamental studies and is important for adhesion and biomedical applications. Postprocessing methods such as plasma and chemical treatments have been used to modify surfaces of a variety of polymers.^{1–4} Modification by surface-initiated graft polymerization and related methods also provides surfaces with tailored functionality.^{5,6} A surface modifying additive (SMA) approach is an attractive alternative for economical surface modification while retaining bulk properties.^{7,8} The importance of the soft block in defining surface composition for polyurethanes^{9–13} has led us to continue exploring novel surface-active soft block compositions and architectures that may be useful in SMAs.

To introduce surface multifunctionality, we have focused on telechelic polyoxetanes [substituted poly(1,3-propylene oxide)diols] with structure **1**, where R_f is a



semifluorinated group and R is a functional group. Recently, we reported the synthesis of novel telechelics with hydrophobic semifluorinated and hydrophilic oligoalkyl ether pendant groups.¹⁴ In this communication, we report the synthesis of oxetane telechelics with hydrophobic semifluorinated and hydrophilic oligoalkyl ether pendant groups having *random* and *block* sequences as well as polyurethanes incorporating these novel soft blocks. The polyurethanes have different nanoscale surface morphologies (TM-AFM) and water contact angles depending on soft segment sequence, again reflecting soft block dominance in determining surface nanostructure.

Ring-opening polymerization of oxetanes is well-known, and several copolyoxetanes have been synthesized.^{15,16} There is uncertainty about molecular weight control (cyclic oligomer formation and likely chain transfer), but we have reported microstructural information on P(ME2Ox-co-5FOx) from a kinetic study of the monomer reactivity ratio ("P" distinguishes monomer from repeat in telechelic).¹⁴ Reaction solvent polarity affected slightly the reactivity ratios, but the monomer distribution in the copolymer was nearly random.

The reaction mechanism of cationic ring-opening polymerization (ROP) of oxetane monomers using boron trifluoride (BF₃) has seen considerable study, and the general features are known.^{15–18} In the present work, modified reaction conditions were used to give telechelics having different monomer sequences.¹⁹ The goal

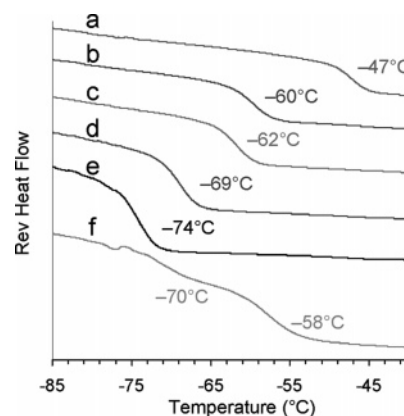
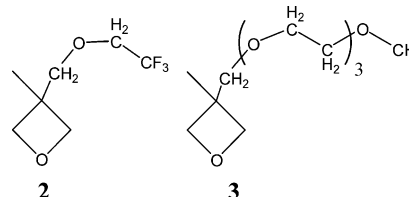


Figure 1. Reversible heat flow curves for polyoxetane telechelics by MDSC (3 °C/min) and modulation amplitude ± 0.5 °C, 30 s: (a) P(3FOx), (b) P(ME3Ox-*block*-3FOx) (2/3, mol/mol), (c) P(ME3Ox-*ran*-3FOx) (1/1), (d) P(ME3Ox-*block*-3FOx) (2/1), (e) P(ME3Ox), and (f) physical mixture of P(ME3Ox) and P(3FOx).

of this work was to learn whether monomer sequence distribution would affect surface properties of derived polyurethanes.



To obtain a blocky-type copolymer, monomer addition order and addition speed were varied. When 3FOx monomer **2** was polymerized first in the presence of BF₃–OEt₂ and butanediol (BD) cocatalysts and the second monomer ME3Ox **3** was added, a two-phase mixture of homotelechelic was obtained. Interestingly, when ME3Ox was added as the first monomer followed by 3FOx, the product was a one-phase viscous liquid, suggesting formation of a block copolymer. After the reaction of first monomer ME3Ox, M_n determined by end group analysis with trifluoroacetic anhydride is 2.6 kg mol^{–1}. Then, after slow addition of 3FOx, a cotelechelic was obtained with $M_n = 4.2$ kg mol^{–1}. A parallel increase in M_w by GPC was obtained.

GPC molecular weight determinations on telechelics usually showed the presence of a peak corresponding to cyclic tetramers (0–20%).²⁰ At present, only qualitative conclusions are drawn from DSC and ¹⁹F NMR data. However, DSC and ¹⁹F NMR data on P[3FOx] from which cyclics were removed are little changed compared with the tetramer-containing product.²¹ Once telechelics are incorporated in polyurethanes, cyclics are removed in reprecipitation as telechelics are nonpolar. Details of separation and analyses will be presented in a full paper.

Figure 1 shows reversible heat flow curves for a series of homo- and cotelechelic obtained by modulated-DSC measurements.²² P(3FOx) and P(ME3Ox) homotelechelic have T_g 's at –47 and –74 °C, respectively (Figure 1a,e). A physical mixture of P(ME3Ox) and P(3FOx) (Figure 1f) shows two T_g 's as the homotelechelic are largely immiscible. DSC data are supported by visual

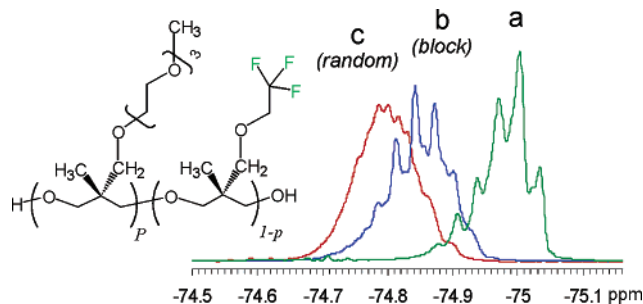


Figure 2. Typical ^{19}F NMR spectra in chloroform- d for (a) P(3FOx), (b) P(ME3Ox-*block*-3FOx), and (c) P(ME3Ox-*ran*-3FOx).

observation of immiscibility when the homotelechelic are mixed. However, partial phase mixing is evident from the T_g shifts relative to pure homotelechelic. The *random* (1:1) cotelechelic T_g is -62°C (Figure 1c), which is close to the average of the homotelechelic. Each *block* telechelic (2:3 and 2:1) also has only one T_g (Figure 1b,d) that approximates the expected average. In summary, the DSC results provide evidence that P(ME3Ox-*block*-3FOx) is not a mixture of homopolymers.

Usually, diblock copolymers comprised of segments forming amorphous domains have two T_g 's.²³ However, Baer has recently shown that, even for high molecular weight glassy polymers, when the scale of phase separation is reduced to a few tens of nanometers, a separate T_g for each phase is not observed.²⁴ Below, we describe nanoscale phase separation for P(ME3Ox-*block*-3FOx) polyurethane surfaces. Perhaps a similar nanoscale phase separation occurs in the bulk *block* telechelics and accounts for the observation of a single T_g 's by DSC.

To substantiate structural differences between *block* and *random* cotelechelic, ^{19}F NMR spectra were ob-

tained (Figure 2).²⁵ The CF_3 - peaks in *block* and *random* telechelics shift by about 0.1–0.2 ppm relative to P(3FOx). A similar small shift is observed when P(ME3Ox) is admixed with P(3FOx) solutions, indicating the shift for copolymers is largely a solvent-like effect.²¹

A comparison of the relative peak shapes is revealing. Homotelechelic and *block* telechelics show a series of well-resolved peaks with $J_{1\text{H}-19\text{F}} = 8\text{ Hz}$. In contrast, the random copolymer peak is broad with little resolvable structure. This observation supports the hypothesis that the random telechelic is comprised of random sequences with many sequence distributions. In contrast, the *block* cotelechelic contains $(3\text{-FOx})_n$ sequences that mimic those in the homotelechelic. Hence, P(3FOx) and P(ME3Ox-*block*-3FOx) have similar ^{19}F NMR spectra.²¹

Polyurethanes were prepared using polyoxetane telechelics or a reference PTMO soft segment.^{26–28} Figure 3 shows the structure and ^1H NMR spectrum of a representative PU, MDI/BD(27)/P(ME3Ox-*ran*-3FOx(1:1)), PU-1 in DMSO- d_6 . Polyurethanes are designated isocyanate/chain extender (hard segment wt %)/soft segment repeat 1-*sequence*-soft segment repeat 2 (mole ratio). Other compositions were also determined by ^1H NMR spectra: MDI/BD(32)/P(ME3Ox-*block*-3FOx(2:3)), PU-2, and MDI/BD(36)/PTMO, PU-3. Glass slides were dip-coated from 20% DMAc solutions.²⁹

TM-AFM was used for evaluating polymer surface morphology.³⁰ Figure 4 shows TM-AFM images (in air) of PU films containing P(ME3Ox-*ran*-3FOx) (PU-1), P(ME3Ox-*block*-3FOx) (PU-2), and PTMO (PU-3). The root-mean-square (rms) height deviation R_q for the area interrogated is commonly used to evaluate the surface roughness. By this measure, surfaces of all films are topologically quite flat (Figure 4a,c,e) with R_q less than 1 nm.

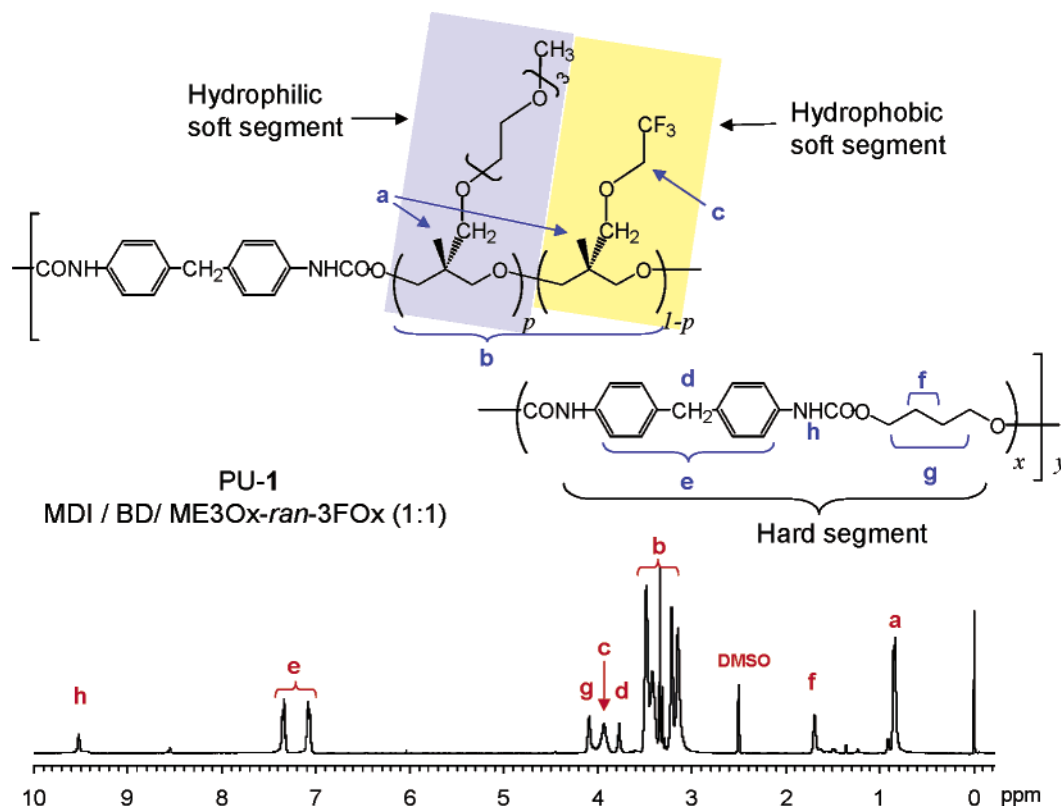


Figure 3. Chemical structure and ^1H NMR spectrum of PU-1 containing P(ME3Ox-*ran*-3FOx) soft segment in DMSO- d_6 .

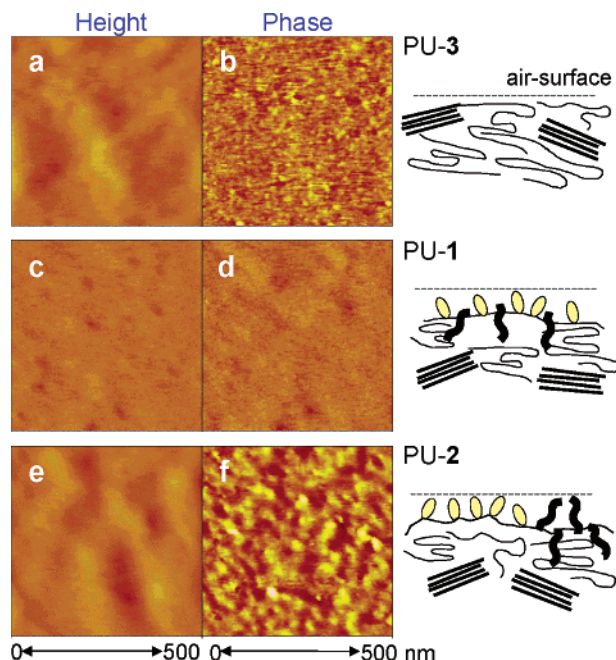


Figure 4. Tapping-mode AFM images of polyurethane films: (a, b) PU-3 (PTMO); (c, d) PU-1, (P(ME3Ox-ran-3FOx)), and (e, f) PU-2, (P(ME3Ox-block-3FOx)). (a, c, e) Height images, $z = 10$ nm. (b, d, f) Phase images, $z = 20^\circ$. R_q : (a) 0.6 nm, (c) 0.3 nm, and (e) 0.9 nm. A/A_0 : (a, b) 0.87, (c, d) 0.83, and (e, f) 0.92.

The surface of PTMO-based PU-3 (Figure 4b) has phase separation on the order of 10 nm due to the hard and soft segments similar to that observed previously.^{11–13} We use a conventional interpretation of modulus-sensitive phase images at light tapping where the lighter color portions are assigned to the organized domain, in this case the MDI–BD hard block. The phase image of P(ME3Ox-ran-3FOx)-based PU-1 is featureless (Figure 4d). This is consistent with a surface structure where the random soft block predominates. With increased tapping force ($A/A_0 = 0.5–0.6$) a phase-separated structure appears in the phase image (not shown), reflecting the presence of near-surface hard blocks.

Importantly, the phase image for P(ME3Ox-block-3FOx)-based PU-2 (Figure 4f) shows strong nanophase separation attributed to ME3Ox and 3FOx domains. By analogy with prior work, the light-colored domains are assigned to the self-organized fluorinated domain.³¹ The average domain size is about 20 nm in diameter, larger than the hard- and soft-segment segregation observed in PU-3 (Figure 4b). The observed phase separation is ascribed to immiscibility and aggregation of P(3FOx) and P(ME3Ox) block segments in the soft phase at room temperature, which is at least 60 °C above the block T_g 's.

The interesting difference in nanoscale surface phase separation for PUs containing *random* and *block* cotelechelic is reflected in contrasting wetting behavior. For evaluation of surface wetting properties, dynamic contact angle (DCA) analysis by the Wilhelmy plate method was used.^{32–34} With R_q less than 1 nm for all coatings, topological roughness is an unlikely contributor to the advancing contact angle (θ_{adv}). However, if selective local swelling occurs in water, θ_{rec} might be affected. Underwater AFM studies are planned.

The DCA results are summarized in Table 1.³⁴ As a point of reference, PU-3 containing the PTMO soft segment was examined: PU-3, θ_{adv} , 93°; θ_{rec} , 49°. From

Table 1. Polyurethane DCA Data

PU soft segment	θ_{adv} (deg)	θ_{rec} (deg)
PU-3 PTMO	93	49
PU-1 P(ME3Ox-ran-3FOx)	104	39
PU-2 P(ME3Ox-block-3FOx)	106	56
homo P(3FOx)	110	70
homo P(ME3Ox)	93	32

previous work^{35,36} and our experience, θ_{adv} , θ_{rec} , and $\Delta\theta$ (44°) are typical values for PTMO PUs. The moderate $\Delta\theta$ (44°) is attributed to rapid surface reorganization of the low- T_g PTMO soft block, though TM-AFM suggests there may be a near-surface hard block contribution as well.

One approach to analysis of chemically heterogeneous surfaces using wetting behavior is to compare an “AB” surface to that of A and B alone. Several well-known methods exist to analyze nonideality responsible for surface behavior.^{37,38} Here, we use a qualitative comparison of cotelechelic PUs with corresponding homotelechelic PUs. Homotelechelic compositions and contact angles are as follows: MDI/BD(29)/P(3FOx): θ_{adv} , 110°, θ_{rec} , 70°; MDI/BD(37)/P(ME3Ox): θ_{adv} , 93°, θ_{rec} , 32°.

Analysis of PU-1 containing P(ME3Ox-ran-3FOx) gave $\theta_{adv} = 104^\circ$, $\theta_{rec} = 39^\circ$, and $\Delta\theta = 65^\circ$.³⁹ The PU-1 surface is hydrophobic in air due to fluorinated groups with θ_{adv} similar to the PU 3FOx homopolymer. However, PU-1 is hydrophilic in water (θ_{rec} , 39°) with a receding contact angle closer to P(ME3Ox) PU (32°) than to P(3FOx) PU (70°). Clearly, extensive surface reorganization occurs in water favoring hydrophilic ether side groups at the water polymer interface. The result is a very large contact angle hysteresis.

For PU-2 containing P(ME3Ox-block-3FOx), θ_{adv} (106°) is also close to θ_{adv} for P(3FOx) PU. In this regard, PU-2 and PU-1 are similar. However, θ_{rec} (56°) is 17° higher than PU-1 (θ_{rec} , 39°), resulting in a smaller contact angle hysteresis for PU-2 (50°) compared to PU-1 (65°). This result indicates the PU-2 surface is hydrophobic in air like P(3FOx) PU and only moderately hydrophilic in water, more like the P(3FOx) PU than P(ME3Ox) PU. Clearly, the nanophase-separated PU-2 surface structure is more hydrophobic overall than the corresponding *random* soft block surface. This amplification of hydrophobicity occurs for PU-2 even though the fluorinated nanodomains do not cover the whole surface (TM-AFM, Figure 4f). Over the limited time scale investigated thus far, the self-assembly responsible for fluorinated surface nanodomains apparently inhibits access of a significant fraction of near-surface, more hydrophilic polyether side chains to water.

Summary. For the first time, the effect of soft block sequence distribution on surface morphology and wetting behavior is demonstrated. Surface nanophase separation is observed for PU-2 containing P(ME3Ox-block-3FOx), while PU-1 containing P(ME3Ox-ran-3FOx) shows no surface microstructure. Interestingly, wetting behavior is influenced by nanoscale surface morphology. This observation suggests that surface nanostructure must be taken into account for demanding applications such as those that require biocompatibility or “smart” behavior.

The extent to which surface properties are retained when PUs such as PU-1 and PU-2 are used in small amounts as SMAs is actively being investigated. Preliminary results suggest that polyurethanes such as PU-1 are highly effective in modifying the surface of conventional polyurethanes.

Acknowledgment. The authors thank the National Science Foundation for research support through Grant DMR-0207560.

References and Notes

- Grace, J. M.; Gerenser, L. J. *J. Dispersion Sci. Technol.* **2003**, *24*, 305–341.
- Olander, B.; Wirsén, A.; Albertsson, A. C. *Biomacromolecules* **2002**, *3*, 505–510.
- Youngblood, J. P.; McCarthy, T. J. *Macromolecules* **1999**, *32*, 6800–6806.
- Chanunpanich, N.; Ulman, A.; Malagon, A.; Strzhemechny, Y. M.; Schwarz, S. A.; Janke, A.; Kratzmueller, T.; Braun, H. G. *Langmuir* **2000**, *16*, 3557–3560.
- Ingall, M. D. K.; Joray, S. J.; Duffy, D. J.; Long, D. P.; Bianconi, P. A. *J. Am. Chem. Soc.* **2000**, *122*, 7845–7846.
- Tsubokawa, N.; Oyanagi, T. *React. Polym.* **1994**, *22*, 47–53.
- Chen, Z.; Ward, R.; Tian, Y.; Malizia, F.; Gracias, D. H.; Shen, Y. R.; Somorjai, G. A. *J. Biomed. Mater. Res.* **2002**, *62*, 254–264.
- Ho, T.; Wynne, K. J. *Polym. Adv. Technol.* **1995**, *6*, 25–31.
- Ratner, B. D.; Cooper, S. L.; Castner, D. G.; Grasel, T. G. *J. Biomed. Mater. Res.* **1990**, *24*, 605–620.
- Andrade, J. D.; Tingey, K. G. *Langmuir* **1991**, *7*, 2471–2478.
- McLean, R. S.; Sauer, B. B. *Macromolecules* **1997**, *30*, 8314–8317.
- Garrett, J. T.; Siedlecki, C. A.; Runt, J. *Macromolecules* **2001**, *34*, 7066–7070.
- Kim, Y. S.; Lee, J. S.; Ji, Q.; McGrath, J. E. *Polymer* **2002**, *43*, 7161–7170.
- Fujiwara, T.; Makal, U.; Wynne, K. J. *Macromolecules* **2003**, *36*, 9383–9389.
- Bucquoye, M.; Goethals, E. J. *Eur. Polym. J.* **1978**, *14*, 323.
- Manser, G. E.; Ross, D. L. In U.S. ONR Report ADA120199: US, 1982.
- Bednarek, M.; Kubisa, P.; Penczek, S. *Macromolecules* **2001**, *34*, 5112–5119.
- Kubisa, P. *J. Polym. Sci., Polym. Chem.* **2003**, *41*, 457–468.
- The oxetane monomer 3-(2,5,8,11-tetraoxadodecyl)-3-methyloxetane (ME3Ox) was synthesized from tri(ethylene glycol) monomethyl ether and 3-bromomethyl-3-methyloxetane (BrOx). Copolymerization of ME3Ox and 3-trifluoroethoxymethyl-3-methyloxetane (3FOx) was carried out by cationic ring-opening polymerization using BF_3 catalyst. For the preparation of P(ME3Ox-*block*-3FOx), ME3Ox was polymerized first at 0 °C for 4 h, and then dilute 3FOx (CH_2Cl_2) was added slowly dropwise for 24 h. The reaction mixture was stirred more 12 h and then quenched with water.
- Malik, A. A.; Archibald, T. G. GenCorp: US, 2000.
- Recently, DSC on P(3FOx) from which cyclics were removed shows a T_g of -48 °C, close to the sample containing 15–20% cyclics. Apparently, P(3FOx) T_g is not very sensitive to the presence of cyclics. ^{19}F NMR peaks for cyclics are at lower field (Figure 2, 74.91, 74.94, and 74.97 ppm) than P(3FOx) and are absent in the ^{19}F NMR spectrum of purified P(3FOx). The intensity of the peaks for cyclics is about 15% of that for P(3FOx). GPC data show that the percent cyclics is consistently lower (0–12%) in cotelecholics containing ME3Ox.
- A TA-QseriesTM (TA Instruments) differential scanning calorimeter (DSC) was used for obtaining glass transition temperatures using modulated-DSC mode from -90 °C at 3 °C/min and modulation amplitude ± 0.5 °C, 30 s.
- Sperling, L. H. *Appl. Polym. Sci.* **2000**, 343–354.
- Liu, R. Y. F.; Jin, Y.; Hiltner, A.; Baer, E. *Macromol. Rapid Commun.* **2003**, *24*, 943–948.
- Chemical structures were established by ^1H NMR (Varian, Inova 400 MHz) and ^{19}F NMR (Varian, Mercury 283 MHz). ^{19}F NMR spectra were obtained in chloroform-*d* using trifluoroacetic acid as an internal reference.
- Polyurethanes were prepared in dimethylacetamide (DMAc) solutions. Methylenediphenyl diisocyanate (MDI) and 1,4-butanediol (BD) were used for hard block. A two-step synthesis (MDI and soft block first) was used. Soft blocks were P(ME3Ox), P(FOx), and P(ME3Ox/3FOx). Poly(tetra-methylene oxide) (PTMO-2000) was used as soft block for a reference polyurethane.
- Grapski, J. A.; Cooper, S. L. *Biomaterials* **2001**, *22*, 2239–2246.
- Bertolucci, M.; Chiellini, E.; Galli, G.; Uilk, J.; Wynne, K. J. *Polym. Prepr.* **2002**, *43*, 647.
- PU coatings were obtained by dip-coating glass slides from 20% dimethylacetamide (DMAc) at room temperature, followed by drying (60 °C, 5 h, ambient pressure; then 80 °C, 2 days, vacuum).
- A Nanoscope-IIIa AFM (Digital Instruments, CA) was used for morphological analysis of PU film surfaces in air. Tapping mode utilized silicon cantilevers.
- Uilk, J.; Johnston, E. E.; Bullock, S.; Wynne, K. J. *Macromol. Chem. Phys.* **2002**, *203*, 1506–1511.
- Gregonis, D. E.; Hsu, R.; Buerger, D. E.; Smith, L. M.; Andrade, J. D. In *Macromolecular Solutions*; Seymour, R. B., Stahl, G. A., Eds.; Pergamon Press: New York, 1982; pp 120–133.
- Uilk, J. M.; Mera, A. E.; Fox, R. B.; Wynne, K. J. *Macromolecules* **2003**, *36*, 3689–3694.
- Dynamic contact angle (DCA) analysis was carried out with a Cahn model 312 analyzer (Cerritos, CA) based on the Wilhelmy plate method. Typically, three cycles were obtained; average error, $\pm 1^\circ$.
- Herbert, C. B.; Hernandez, A. M.; Hubbell, J. A. *Biotechnol. Bioeng.* **1996**, *52*, 81–88.
- Lamba, N. M. K.; Woodhouse, K. A.; Cooper, S. L. In *Polyurethanes in Biomedical Applications*; CRC Press: Boca Raton, FL, 1998; p 15.
- Johnson, R. E., Jr.; Dettre, R. H. In *Surfactant Science Series*; Berg, J. C., Ed.; M. Dekker: New York, 1993; Vol. 49, pp 1–73.
- Neumann, A. W.; Good, R. J. *J. Colloid Interface Sci.* **1972**, *38*, 341–358.
- Water contamination required use of a large area water reservoir to obtain reproducible (two cycles) advancing and receding contact angles.

MA048747N